IEEE Journal of Translational Engineering in Health and Medicine

Received 15 October 2018; revised 23 December 2018 and 4 February 2019; accepted 4 February 2019. Date of publication 11 April 2019; date of current version 21 May 2019.

Digital Object Identifier 10.1109/JTEHM.2019.2898870

Context Dependent Fuzzy Associated Statistical Model for Intensity Inhomogeneity Correction From Magnetic Resonance Images

BADRI NARAYAN SUBUDHI[1], T. VEERAKUMAR[2], S. ESAKKIRAJAN[3], AND ASHISH GHOSH[4]

[1]Department of Electrical Engineering, Indian Institute of Technology Jammu, Jammu 181221, India
[2]Department of Electronics and Communication Engineering, National Institute of Technology, Goa 403401, India
[3]Department of Instrumentation and Control Engineering, PSG College of Technology, Coimbatore 641004, India
[4]Machine Intelligence Unit, Indian Statistical Institute, Kolkata 700105, India

CORRESPONDING AUTHOR: T. VEERAKUMAR (tveerakumar@yahoo.co.in)

This work was supported by SERB, India, under Grant EMR/2016/002552.

ABSTRACT In this paper, a novel context-dependent fuzzy set associated statistical model-based intensity inhomogeneity correction technique for magnetic resonance image (MRI) is proposed. The observed MRI is considered to be affected by intensity inhomogeneity and it is assumed to be a multiplicative quantity. In the proposed scheme the intensity inhomogeneity correction and MRI segmentation is considered as a combined task. The maximum a posteriori probability (MAP) estimation principle is explored to solve this problem. A fuzzy set associated Gibbs' Markov random field (MRF) is considered to model the spatio-contextual information of an MRI. It is observed that the MAP estimate of the MRF model does not yield good results with any local searching strategy, as it gets trapped to local optimum. Hence, we have exploited the advantage of variable neighborhood searching (VNS)-based iterative global convergence criterion for MRF-MAP estimation. The effectiveness of the proposed scheme is established by testing it on different MRIs. Three performance evaluation measures are considered to evaluate the performance of the proposed scheme against existing state-of-the-art techniques. The simulation results establish the effectiveness of the proposed technique.

INDEX TERMS Markov random field, intensity inhomogeneity, fuzzy clustering, maximum a posteriori probability.

I. INTRODUCTION

In the last few decades the use of Magnetic Resonance (MR) imaging has tremendously increased due to its capability in extracting meaningful information from a human body in a non-invasive manner. The use of information from the MR images helps in diagnosis, therapy planning, and monitoring of the patient for further treatments [1]. One of the common problems in MRI medical image analysis is spatial intensity inhomogeneity induced by the radio-frequency coil of the MR imaging device during MRI acquisition process. Removal of intensity inhomogeneity from MRI is a difficult task and is a major problem to be solved in medical imaging domain. This is usually referred to as intensity inhomogeneity, intensity non-uniformity, shading or bias field [2]. In the MR image the intensity inhomogeneity appears as a slowly varying quantity and is tissue independent. Early work for intensity inhomogeneity estimation is proposed using phantom based approach [3]. Homomorphic unsharp filtering [4] is also studied for intensity inhomogeneity correction. It may be noted that both phantom and homomorphic unsharp filtering are deterministic approaches. Hence better results can be expected using statistical estimation scheme for intensity inhomogeneity correction [5].

A maximum likelihood estimation scheme using Expectation Maximization (EM) algorithm is proposed by Guillemaud and Brady [5] for intensity inhomogeneity correction. Likar *et al.* [6] also suggested an intensity inhomogeneity correction technique, where the intensity inhomogeneity affected MRI is described by a linear model, consisting of multiplicative and additive components of smoothly varying basis functions. Sled *et al.* [7] also suggested an iterative N3 scheme of intensity inhomogeneity correction technique

which is a non-parametric approach and does not need a model of the tissue classes in the MRI. A modification of N3 approach is also studied by Tustison *et al.* [8], where the B-spline approximation algorithm with modified optimization strategy is used to capture a range of bias modulation.

Most of the approaches in the literature assumed that segmentation and intensity inhomogeneity estimation are combined process and different segmentation techniques are explored. Dawant *et al.* [9] proposed an intensity inhomogeneity estimation scheme where some manually selected points from the white matter in the brain are fitted with the least-squares spline and are used further. Meyer *et al.* [10] also suggested a scheme where the intensity inhomogeneity is estimated from the intermediate segmentation of MRIs. Li *et al.* [11] proposed a technique where the authors have designed a local clustering criterion for the intensities at the neighborhood of each point. Recently, Li *et al.* [12] also studied an intensity inhomogeneity estimation scheme where the intensity inhomogeneity is iteratively optimized by using efficient matrix computations popularly known as multiplicative intrinsic component optimization (MICO). Recently, Ivanovska *et al.* [13] proposed a novel algorithm for simultaneous segmentation and intensity inhomogeneity correction, where the energy functional allows for explicit regularization of the intensity inhomogeneity term, making the model more flexible in presence of strong inhomogeneities.

Among all the segmentation schemes, fuzzy clustering based techniques [14] are widely adopted for this task. Xu *et al.* [15] proposed an adaptive fuzzy clustering scheme where the segmentation and intensity inhomogeneity compensation are considered as a combined task. A modified fuzzy clustering based intensity inhomogeneity estimation is proposed by Pham and Prince [16] where the developed objective function tried to include the multiplier field and estimate the intensity inhomogeneity. Ahmed *et al.* [17] also suggested an intensity inhomogeneity estimation technique where the objective function of the standard FCM algorithm is modified with the neighborhood information so as to compensate the inhomogeneities in MRIs. A fast and robust FCM clustering algorithm incorporating local information is also suggested by Cai *et al.* [18] for image segmentation, which is found to be efficient and faster. It may be observed that the performance of clustering is further improved using kernel techniques [19]. The possibillistic FCM clustering is also explored in this regard [20]. Here it is required to mention that in pixel based approaches, use of probabilistic/deterministic models may not consider the contextual information. Markov random field (MRF) [21], a statistical model, is found to be effective and convenient for modeling the contextual features of images such as, edge, gray value, color, texture, etc. MRF integrates the mutual influence of neighboring pixels in conditional probability prior. An extension of Gibbs' distribution with hidden Markov random field (HMRF) is also used for intensity inhomogeneity correction where tissue parameters are obtained using penalized likelihood approach [22].

In this article, an efficient intensity inhomogeneity correction technique is proposed. Here simultaneous segmentation and intensity inhomogeneity correction of MRIs are considered. The segmentation problem is considered as white/grey matter separation. A fuzzy set associated Gibbs' MRF is considered to model the spatial gray level attributes of the MRI. A resemblance between the MAP estimate of the MRF and the spatio-contextual fuzzy clustering objective function is identified. The maximum *a posteriori* probability (MAP) estimation principle is employed to solve the combined problem of intensity inhomogeneity correction and segmentation. It is observed that the MAP estimate of the MRF model does not yield good solutions by any gradient descent based local searching strategy, as it may get trapped to local optimum. Hence, we have explored the advantage of variable neighborhood searching (VNS) based iterative global convergence criterion for MRF-MAP estimation.

The organization of this paper is as follows. Section II describes an overview of the proposed technique with detailed block diagram. The intensity inhomogeneity correction results are analyzed in Section III. Finally, in Section IV conclusions of this work are drawn.

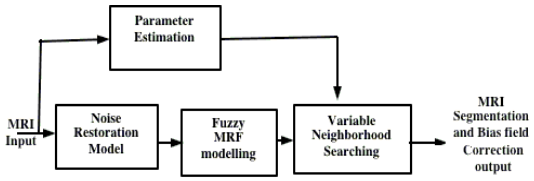

FIGURE 1. Block diagram of the proposed scheme.

II. PROPOSED FUZZY SET ASSOCIATED GIBBS' MARKOV RANDOM FIELD FOR MRI SEGMENTATION AND INTENSITY INHOMOGENEITY ESTIMATION

A block diagram of the proposed method is given in Fig. 1. In the proposed scheme the intensity inhomogeneity affected image is considered as the input to the system. The input image is assumed to be affected by intensity inhomogeneity which is considered as a multiplicative noise and the noise restoration model is considered as a logarithmic additive process. Here the intensity inhomogeneity correction and MRI segmentation is considered as a common problem. In the next step of processing, considered MRI is modeled with a fuzzy-statistics based Gibbs' MRF. The combined problem of intensity inhomogeneity correction and segmentation is considered as a MAP estimation problem. The variable neighborhood searching scheme with the expectation maximization (EM) algorithm is explored for estimating the MAP and the parameters of the MRF model. In the next sub sections, we describe the MRF-MAP framework and the proposed spatio-contextual fuzzy clustering schemes, which is the basis for the proposed intensity inhomogeneity correction technique.

IEEE Journal of Translational Engineering in Health and Medicine

A. NOISE RESTORATION MODEL FOR INTENSITY INHOMOGENEITY CORRECTION

The considered MRI is assumed to come from an imperfect imaging modality. It is assumed that noise has corrupted the actual image d to produce the observed image g. Given this observed image g, we seek the actual noise free image d, which is corrupted by intensity inhomogeneity H and additive noise N. Hence g can be expressed as

$$g = Hd + N. \tag{1}$$

The noise is considered to follow Rician distribution [1], which is quasi-Gaussian at high signal-to-noise ratio. Hence in our work, we have considered the noise as Gaussian distributed with zero-mean. Rician noise has a positive mean, and the estimator will be a biased estimator. Generally, the effect of the additive noise component is a linear one and can be filtered out as the amount of noise component in MRIs is less significant than the effect of the multiplicative component. Use of a logarithmic transformation on both sides of the above equation allows the expression to be modeled as an additive intensity inhomogeneity model represented by:

$$y = u + b, \tag{2}$$

where y and u are the logarithmic transform of the observed (g) and the true (d) intensities of MRI, respectively, and b is the log-transformed intensity inhomogeneity (H). Here noise is assumed to be a multiplicative intensity inhomogeneity (H). Most of the literature on intensity inhomogeneity correction assumed the MRI segmentation and intensity inhomogeneity correction as a combined iterative procedure. Fuzzy clustering [14] and MRF based approaches are separately used in this context. In the proposed scheme, we have considered fuzzy set associated MRF model for intensity inhomogeneity correction.

B. GIBBS' MARKOV RANDOM FIELD MODEL FOR SOLVING THE COMBINED PROBLEM OF MRI SEGMENTATION AND INTENSITY INHOMOGENEITY CORRECTION

The proposed scheme is considered as a combined task of solving the intensity inhomogeneity correction and segmentation. We start our approach as the task of segmenting the noisy MRI y for estimating and correcting the intensity inhomogeneity of the input MRI. Here the segmentation problem is considered as white/grey matter separation. In the proposed scheme, we assumed the f-dimensional MRI as a contextual entity and denoted it by y. It is assumed that each pixel in y is a site denoted by s, where $s \in S$, and $S = M \times N$ is the set of all sites. y is considered as a realization of random field Y. X is considered as a random variable and x is a realization of it. $\mathrm{X} = x$ is a partition of the image into different K region types, i.e., $x \in \{q_1, q_2, \ldots\}$ is a generic set of K labels or cluster prototypes assigned to the pixels in y, where q_i corresponds to different region types. In essence x is the segmentation of y. We have considered y as the observation and x as the label field which is supposed to be estimated. Different classes are assumed to be spatially disjoint.

Here X is considered as an MRF, hence the Markovianity property [22] is satisfied in spatial direction, i.e.,

$$\begin{aligned} \mathrm{P}(\mathrm{X}_s = \mathrm{x}_s | X_r = \mathrm{x}_r, \forall r \in \mathrm{S}, \mathrm{s} \neq r) \\ = \mathrm{P}(\mathrm{X}_s = \mathrm{x}_s | X_r = \mathrm{x}_r, \mathrm{r} \in \eta_s), \end{aligned} \tag{3}$$

where η_s denotes the neighborhood of s in S.

Here the combined problem of intensity homogeneity correction and segmentation are considered to be a process of estimating x that has given rise to the MRI y. This is possible by statistically estimating $\hat{x}$ from y. This can be obtained by

$$\hat{x} = \arg\max_x \frac{P(Y = y|X = x)P(X = x)}{P(Y = y)}, \tag{4}$$

where $\hat{x}$ is the estimated labels. Here y is the given input MRI and P(Y=y) is constant. Hence eq (4) will take the form

$$\hat{x} = \arg\max_x \{P(Y = y|X = x, \theta)P(X = x, \theta)\}, \tag{5}$$

where θ is the parameter vector and $\mathrm{P}(X = x, \theta)$ is the prior probability and $\mathrm{P}(Y = y|X = x, \theta)$ is the likelihood function.

It may not be possible to calculate the above probability directly, as it considers conditional dependency among the pixels. Hammersley-Clifford theorem [21] with Pott's theory [22] gives a convenient way to express them. As per Hammersley-Clifford theorem, the joint probability $P(X = x, \theta)$ can be considered to be a Gibbs' distribution as

$$P(X = x, \theta) = \prod_{c \in C} \psi(x), \tag{6}$$

where c represents the clique and C is the set of cliques. Here we have considered second order cliques for the analysis. The energy prior function $\psi(x)$, can be described as,

$$\psi(x) = \frac{1}{z} e^{-\frac{U(x)}{T}} = \frac{1}{z} e^{-\frac{\left\{\left(-\sum_{c \in C} V_c(x)\right)\right\}}{T}}, \tag{7}$$

and the partition function z is expressed as $z = \sum_x e^{\frac{-U(x)}{T}}$, $U(x)$ is the energy function. T is the temperature constant. In eq (7), $V_c(x)$ represents the clique potential function and can be defined as

$$\mathrm{V}_c(\mathrm{x}) = \begin{cases} +\alpha & \text{if } \mathrm{x}_s = \mathrm{x}_r \\ -\alpha & \text{if } \mathrm{x}_s \neq \mathrm{x}_r \end{cases}, \tag{8}$$

where α is the MRF model bonding parameter and s and r are two neighboring sites.

The likelihood function $\mathrm{P}(Y = y|X = x, \theta)$ is considered to follow Gaussian distribution. Accordingly, the parameter vector θ can be described as, $\theta = \{\sum_j, \mu_j, \pi_{ij}\}$, where μ_j, $\sum_j$ and π_{ij} represent the mean, variance and the point-wise prior probabilities of the MRF for i^{th} site being in the j^{th} cluster, respectively.

Thus, the likelihood function $P(Y = y|X = x, \theta)$ can be expressed as,

$$\begin{aligned} &P(X = x, \theta) \\ &= \prod_{i=1}^{M\times N} P(Y_i = y_i|X_i = j, \theta) \\ &= \prod_{i=1}^{M\times N} \frac{1}{\sqrt{(2\pi)^f \det[\sum_j]}} e^{-\frac{1}{2}(u_i-b_i-\mu_j)^T \sum_j^{-1}(u_i-b_i-\mu_j)}. \end{aligned} \quad (9)$$

In the above expression we have considered $y = u + b$, as explained in eq (2), and each pixel or site in u and b is represented as u_i and b_i. The parameter f is the number of features used for analysis of the observed image. Considering the prior probability of MRF and the likelihood function as in eq (9), the posterior probability of MRF is written as

$$\hat{x} = \arg\max_x \sum_{i=1}^{M\times N} A - \left[\frac{1}{2}(u_i - b_i - \mu_j)^T \sum_j^{-1} (u_i - b_i - \mu_j)\right] - \sum_{c\in C} V_c(x), \quad (10)$$

where $A = -\frac{1}{2}\log\left((2\pi)\det\left[\sum_j\right]\right)$ is a constant and $\hat{x}$ is the MAP estimate. It may be noted that such an approximation is expected to be a crisp. Hence we have modified the above equation by considering a soft version of the above expression.

C. FUZZY STATISTICS BASED MARKOV RANDOM FIELD AND CORRESPONDING MAP ESTIMATION

An MRI is usually altered by real life vagueness and uncertainty. Hence the use of a deterministic framework may not be able to give a better solution in this regard. Fuzzy sets [23] are popular and powerful tools in this context and are found to provide satisfactory results. Integration of fuzzy sets with MRF model plays tremendous role in detecting the boundaries corresponding to different matters in an MRI.

In the proposed scheme, we have considered a modified form of the MRF model for MAP estimation. We adhered to the regularized fuzzy statistic based MRF-MAP model. In the proposed scheme, the MRF-MAP framework is considered as a fuzzy objective function which intends to cluster the MRI into K partitions, where K is the number of clusters. Incorporating the bias field restoration process in the above equation we may obtain (11), as shown at the bottom of this page, where m_{ij} is the membership function for site i^{th} belong to the j^{th} cluster. Here π_{ij} is the prior probability and K represents the number of clusters. This will be further reduced to the form

$$\begin{aligned} J_m = &-\sum_{i=1}^{M\times N}\sum_{j=1}^{K} m_{ij}\frac{1}{2}\log\left((2\pi)^f \det\left[\sum_j\right]\right) \\ &- m_{ij}\left[\frac{1}{2}\left(u_i - b_i - \mu_j\right)^T \sum_j^{-1}\left(u_i - b_i - \mu_j\right)\right] \\ &+ \lambda\sum_{i=1}^{M\times N}\sum_{j=1}^{K} m_{ij}\left\{\log\left(m_{ij}\right) - \left[\sum_{c\in C} V_c(x)\right]\right\}. \end{aligned} \quad (12)$$

This needs estimation of the parameters μ_j and $\sum_j$. EM algorithm is used with Variable Neighborhood Searching (VNS) framework for this purpose.

D. VARIABLE NEIGHBORHOOD SEARCHING

The conventional FCM iterative scheme follows a random selection of the cluster centers. It updates the cluster centers by optimizing the fuzzy objective function. However, it may get stuck to local minima. It may be noted from the literature, that variable neighbor searching (VNS) based optimization [24], a meta-heuristic optimization scheme, and produces better solutions against the conventional FCM. Hence in the proposed work, we adhered to the VNS based optimizing scheme for optimizing the MRF-FCM optimization function.

In the initial stage of the algorithm the number of clusters C is defined. The objective function as expressed in eq (12) is calculated. Then step by step, conventional FCM clustering is iterated to find a new estimate of the variables π_{ij}, μ_j and m_{ij} according to eqs (13-17). The objective function $J_{opt} = J_m$ is also updated according to eq (11) and the neighborhood structure is explored for a new data point with VNS scheme. The suitability of the selected point is checked by the considered MAP function. Then the conventional local FCM search is used to obtain a new mean. The MAP of J_m is obtained and checked. If $J_m < J_{opt}$, the old cluster centers are updated with the obtained new ones and J_{opt} is updated to $J_{opt} = J_m$, else the previous cluster centers and J_{opt} remain the same. Likewise the VNS scheme is repeated over larger neighborhood size until the complete search space is explored.

$$\begin{aligned} J_m = -\sum_{j=1}^{K} m_{ij} \times \log\left\{\prod_{i=1}^{M\times N}\frac{1}{\sqrt{(2\pi)^f \det\left[\sum_j\right]}} e^{-\frac{1}{2}(u_i-b_i-\mu_j)^T \sum_j^{-1}(u_i-b_i-\mu_j)}\right\} \\ + \lambda\sum_{i=1}^{M\times N}\sum_{j=1}^{K} m_{ij}\log\left(\frac{m_{ij}}{\pi_{ij}}\right), \end{aligned} \quad (11)$$

IEEE Journal of Translational Engineering in Health and Medicine

E. PARAMETER ESTIMATION

For an estimation of $x_{ij} \in \{q_1, q_2, \ldots\}$, the incomplete data y is modeled with an MRF. We have used EM algorithm for estimation of the parameter θ [22]. The algorithm starts with an initial random value $\theta^{(o)}$, and at iteration γ, the parameter vector is estimated to $\theta^{(\gamma)}$.

We estimate the point-wise prior probability of the MRF model as

$$\pi_{ij}^{(\gamma+1)} = \frac{e^{\frac{-\sum_{c\in C} V_c(x^{(\gamma)})}{T}}}{\sum_{x^{(\gamma)}} e^{\frac{-\sum_{c\in C} V_c(x^{(\gamma)})}{T}}}, \tag{13}$$

The estimate of x at step γ is obtained by

$$x_j^{(\gamma)} = \arg\max_{j\in Q} \left\{ m_{ij}^{(\gamma)} \right\}, \tag{14}$$

where $m_{ij}^{(\gamma)}$ denotes the fuzzy membership function of the i^{th} site belongs to the j^{th} cluster. At the $(\gamma+1)^{th}$ iteration, the fuzzy membership function can be obtained as

$$m_{ij}^{(\gamma+1)} = \frac{\pi_{ij}^{(\gamma)} \exp\left(-\left(\frac{1}{\lambda}\right) \log\left(P\left(Y=y|X=x,\theta\right)\right)^{(\gamma)}\right)}{\sum_{l=1}^{K} \pi_{il}^{(\gamma)} \exp\left(-\left(\frac{1}{\lambda}\right) \log\left(P\left(Y=y|X=x,\theta\right)\right)^{(\gamma)}\right)}. \tag{15}$$

The dissimilarity function $\log\left(P\left(Y=y|X=x,\theta\right)\right)^{(\gamma)}$ can be written as

$$\begin{aligned}\log\left(P\left(Y=y|X=x,\theta\right)\right)^{(\gamma)} &= \frac{M\times N}{2}\log(2\pi) + \frac{1}{2}\log\left|\sum_{j}^{(\gamma)}\right| \\ &+ \left[\frac{1}{2}\left(u_i - b_i - \mu_j^{(\gamma)}\right)^T \sum_{j}^{(\gamma)^{-1}} \left(u_i - b_i - \mu_j^{(\gamma)}\right)\right],\end{aligned} \tag{16}$$

where $\sum_j^{(\gamma)}$ represents the covariance of the j^{th} class at the γ^{th} iteration. The mean vector for each cluster is obtained as

$$\mu_j^{(\gamma+1)} = \frac{\sum_{i=1}^{M\times N} m_{ij}^{(\gamma)} (u_i - b_i)}{\sum_{i=1}^{M\times N} m_{ij}^{(\gamma)}}. \tag{17}$$

III. RESULTS AND DISCUSSIONS

This section is divided into three sub-sections. At first visual analysis of results with different existing state-of-the-art techniques are made. In the second part, the same has been evaluated using three different evaluation measures. A discussion on the proposed scheme is carried out in the last part. The algorithm is implemented in $C++$ and is run on Pentium D, 2.8 GHz PC with 2G RAM and Ubuntu operating system. The proposed method is tested on different MRIs from four different benchmark databases: BRAINWEB [25], 4RTNI@LONI [26], customized simulated BRAINWEB [27] and 3T MRI data from NCI-ISBI *2013* Challenge [28]. The performance of the proposed scheme is demonstrated in this article by using seventeen MRIs: ten are taken from "BrainWeb: Anatomical Model of MS Lesion Brain" (one visual and ten analytical), six are taken from "4RTNI$@$LONI" (one visual and six analytical), and one MRIs are taken with 3T from NCI-ISBI+2013+Challenge: T3:1 and T3:14 (one visual). The proposed scheme is validated by comparing the results obtained by it with those of the information minimization (Emin) [6], N3 [7], N4 [8], modified FCM [17], level set [11] and MICO [12] techniques. To have a quantitative evaluation of the proposed scheme, three non-ground-truth based evaluation measures were considered: coefficient of variation of white matter, coefficient of variation of gray matter and coefficient of joint variation.

A. VISUAL ANALYSIS OF RESULTS

The output of the images used for our analysis with comparison against the state-of-the-art techniques are depicted in Figs. 2-4. The three images reported here are Anatomical Model of MS Lesion Brain: BRAINWEB59 data, 4RTNI@LONI: Canvas 30 data and *3T MRI data from NCI-ISBI 2013 Challenge:* T3-01 data.

The first example considered for our experiment is BRAINWEB59 and are shown in Fig. 2. The original intensity inhomogeneity affected image is shown in first row of Fig. 2(a). The intensity inhomogeneity corrected images obtained by different existing state-of-the-art techniques: Entropy Min, N3, N4, level set, modified FCM, MICO and the proposed schemes are shown in first row of Figs. 2(b)-(h). The results obtained by Entropy minimization, N3 and N4 approaches are shown in the first row of Figs. 2(b)-(d). These approaches provided results having low frequency or the smoothed components are attenuated, and hence the corrected MRIs appeared to be granular. It also may be observed that the results obtained by the level set and modified FCM schemes are unable to give good impression in intensity inhomogeneity correction. From these results it may be observed that during intensity inhomogeneity corrections information are lost from bias field corrected MRIs and the results are found to be smoother. The results obtained by MICO scheme is shown in first row of Fig. 2(g). It may be observed from this image that better results of intensity inhomogeneity correction is obtained by MICO scheme as compared to the level set and the modified FCM scheme. However, the results obtained by the proposed scheme is found to be providing better intensity inhomogeneity corrected MRI as compared to the other schemes. The intensity inhomogeneity or the noisy image obtained by all these considered schemes are shown in second row of Fig. 2(b)-(h). The efficiency of intensity inhomogeneity corrections can also be demonstrated

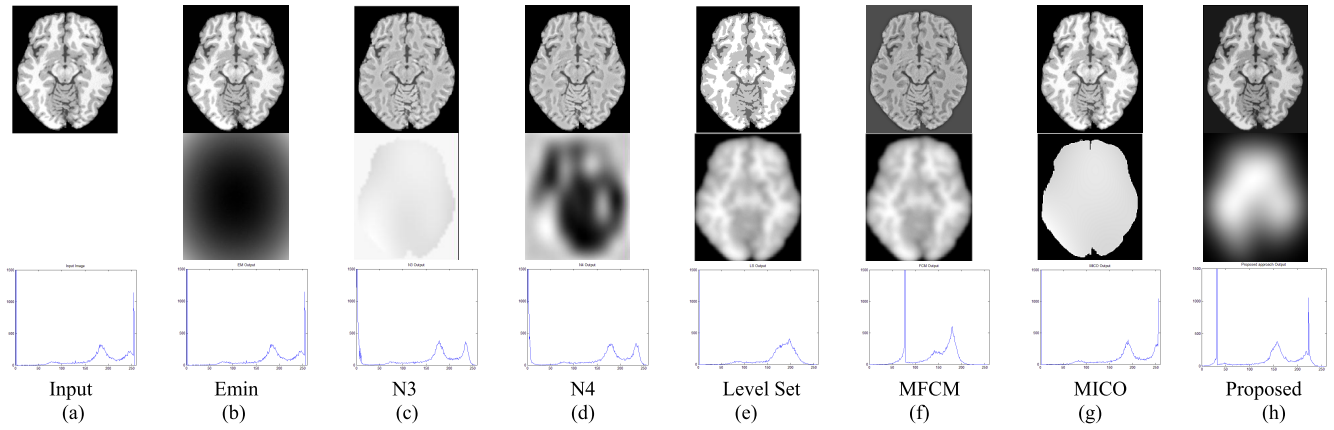

FIGURE 2. Intensity inhomogeneity correction for BRAINWEB59 Data: Row 1: Intensity inhomogeneity corrected MRIs, Row 2: Estimated intensity inhomogeneity, Row 3: Histogram plot. (a) Input. (b) Emin. (c) N3. (d) N4. (e) Level Set. (f) MFCM. (g) MICO. (h) Proposed.

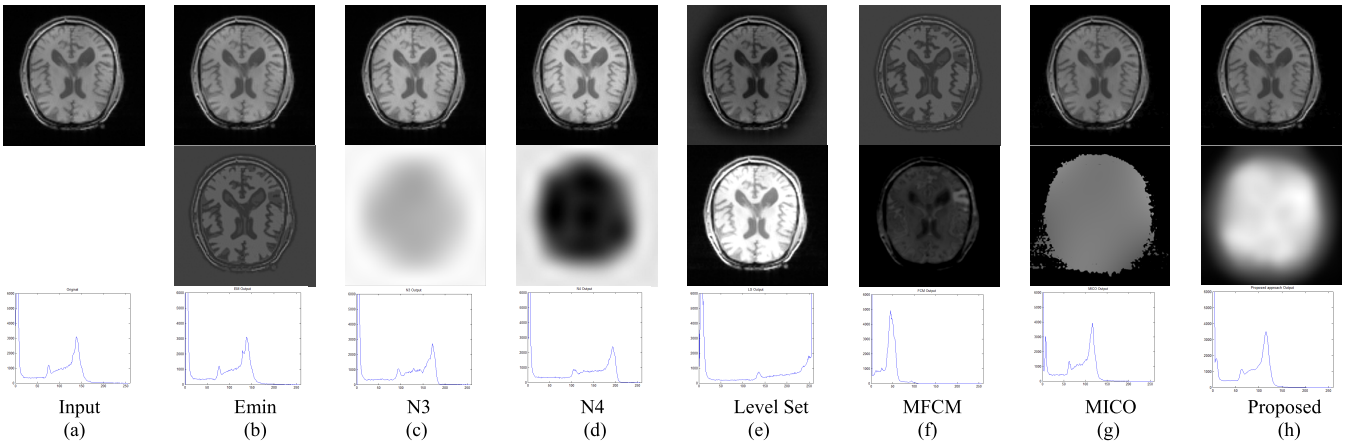

FIGURE 3. Intensity inhomogeneity correction for Canvas30 Data: Row 1: Intensity inhomogeneity corrected MRIs, Row 2: Estimated intensity inhomogeneity, Row 3: Histogram plot. (a) Input. (b) Emin. (c) N3. (d) N4. (e) Level Set. (f) MFCM. (g) MICO. (h) Proposed.

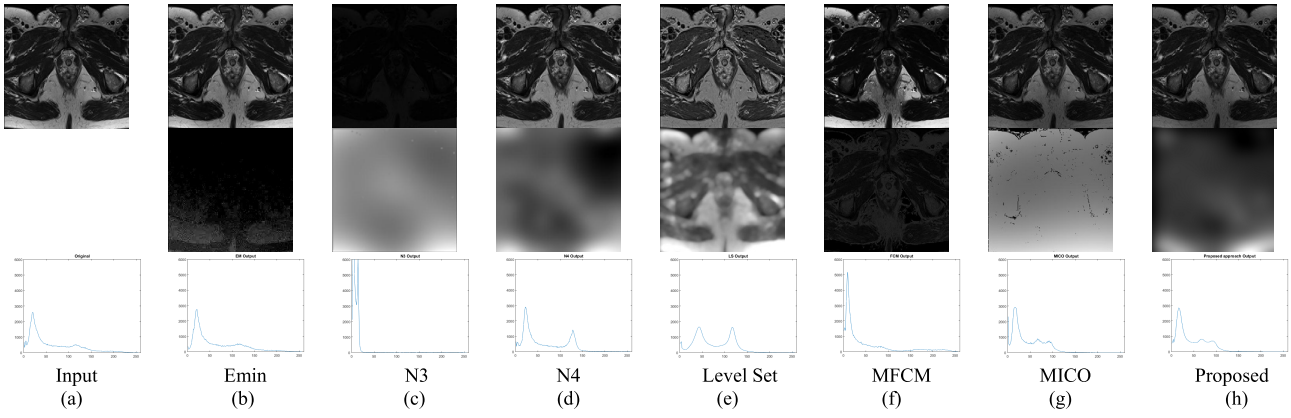

FIGURE 4. Intensity inhomogeneity correction for T3-01 data: Row 1: Intensity inhomogeneity corrected MRIs, Row 2: Estimated intensity inhomogeneity, Row 3: Histogram plot. (a) Input. (b) Emin. (c) N3. (d) N4. (e) Level Set. (f) MFCM. (g) MICO. (h) Proposed.

by comparing the histograms of the original images and the bias corrected images. The distinct and well separated peaks of the intensity inhomogeneity corrected image indicate a better output. Distinct valley implies that the gray levels corresponding to different regions are well separated. Histograms for the original MRI and intensity inhomogeneity corrected images obtained by the considered techniques and the proposed scheme are shown in third row of Figs. 2(b)-(h).

IEEE Journal of Translational Engineering in Health and Medicine

TABLE 1. Performance evaluation measures for brainweb: anatomical model of MS lesion brain data.

Techniques	BRAINWEB59			BRAINWEB64			BRAINWEB72			BRAINWEB79			BRAINWEB-axial-89		
	CV(GM)	CV(WM)	CJV	CV(GM)	CV(WM)	CJV	CV(GM)	CV(WM)	CJV	CV(GM)	CV(WM)	CJV	CV(GM)	CV(WM)	CJV
Original	0.1656	0.0836	1.0036	0.2077	0.1050	1.3113	0.2125	0.1059	1.2927	0.2135	0.1125	1.2342	0.1781	0.0716	0.7914
EMin	0.1656	0.0836	1.0026	0.2077	0.1050	1.3113	0.2125	0.1059	1.2927	0.2100	0.1079	1.2136	0.1781	0.0716	0.7914
N3	0.1616	0.0813	0.9972	0.1839	0.0769	0.9993	0.2094	0.1033	1.3178	0.2103	0.1066	1.2072	0.1750	0.0650	0.7943
N4	0.1607	0.0798	1.0118	0.1894	0.0828	1.0927	0.2084	0.1029	1.3553	0.2112	0.1081	1.2293	0.1788	0.0670	0.7874
MFCM	0.1487	0.0757	2.0558	0.1650	0.0697	1.9492	0.1714	0.0953	2.9824	0.1782	0.0912	2.4493	0.1664	0.0712	1.5482
LSE	0.1359	0.0708	1.8798	0.1542	0.0667	1.8620	0.1863	0.0884	2.8075	0.1871	0.0887	2.2752	0.1577	0.0674	1.6197
MICO	0.1621	0.0808	0.9967	0.1818	0.0796	1.0133	0.2092	0.1019	1.3439	0.2093	0.1065	1.2132	0.1728	0.0619	0.7921
Proposed	**0.1206**	**0.0684**	**0.9028**	**0.1566**	**0.0592**	**0.9232**	**0.1694**	**0.0859**	**1.1602**	**0.1629**	**0.0728**	**1.0986**	**0.1494**	**0.0585**	**0.5027**

TABLE 2. Performance evaluation measures for "4RTNILONI" data

Techniques	Canvas			Canvas 30			Canvas 45		
	CV(GM)	CV(WM)	CJV	CV(GM)	CV(WM)	CJV	CV(GM)	CV(WM)	CJV
Original	0.2065	0.1924	1.6225	0.1998	0.1057	1.1092	0.1992	0.0528	0.8826
EMin	0.1899	0.1409	1.6009	0.1802	0.1025	1.0061	0.1905	0.0606	0.8525
N3	0.1861	0.1329	1.4965	0.1794	0.1004	1.0009	0.1816	0.0492	0.8496
N4	0.1859	0.1290	1.5224	0.1690	0.0981	0.9826	0.1794	0.0481	0.8391
MFCM	0.1942	0.1465	2.3618	0.1629	0.0892	2.0904	0.1881	0.0516	1.6295
LSE	0.1728	0.1124	1.8841	0.1602	0.0860	1.2952	0.2019	0.0506	1.7228
MICO	0.1704	0.1053	1.3075	0.1571	0.0725	0.9622	0.1699	0.0461	0.8199
Proposed	**0.1662**	**0.0992**	**1.1921**	**0.1508**	**0.0695**	**0.9596**	**0.1605**	**0.0409**	**0.7906**

TABLE 3. Performance evaluation measures for other brainweb: anatomical model of MS lesion brain data.

Techniques	BRAINWEB78			BRAINWEB97			BRAINWEB127			BRAINWEB135			BRAINWEB147		
	CV(GM)	CV(WM)	CJV	CV(GM)	CV(WM)	CJV	CV(GM)	CV(WM)	CJV	CV(GM)	CV(WM)	CJV	CV(GM)	CV(WM)	CJV
Original	0.1812	0.1110	1.0119	0.2926	0.1016	1.2880	0.3011	0.1132	1.2790	1.5651	0.0936	1.0046	0.1147	0.0877	0.9113
EMin	0.1765	0.1107	1.0008	0.2956	0.1012	1.2750	0.3001	0.1131	1.5165	1.5611	0.0911	1.0036	0.1131	0.0870	0.9103
N3	0.1746	0.1016	0.9132	0.2923	0.0987	1.2630	0.2987	0.1116	1.5016	1.5601	0.0908	1.0031	0.1110	0.0850	0.9089
N4	0.1689	0.1000	0.9001	0.2918	0.0917	1.2510	0.2966	0.1088	1.4822	1.5587	0.0901	1.0028	0.1103	0.0813	0.9013
MFCM	0.1632	0.0956	0.8987	0.2967	0.0922	1.2720	0.2931	0.1016	1.4765	1.5577	0.0888	1.0021	0.1087	0.0787	0.8922
LSE	0.1616	0.0916	0.8976	0.2915	0.0902	1.2310	0.2916	0.1003	1.4745	1.5565	0.0881	1.0019	0.1055	0.0761	0.8833
MICO	0.1589	0.9660	0.8765	0.2908	0.0931	1.2760	0.2973	0.1011	1.4913	1.5566	0.0906	1.0029	0.1104	0.0860	0.9093
Proposed	**0.1557**	**0.0878**	**0.8555**	**0.2889**	**0.0811**	**1.1970**	**0.2919**	**0.1001**	**1.0000**	**1.5011**	**0.0877**	**1.0001**	**0.1005**	**0.0656**	**0.8517**

It may be observed that three distinct peaks are obtained in the histogram of the proposed intensity inhomogeneity corrected image and are well separated too as compared to the other techniques.

The next example considered for our experiment is canvas 30 data as shown in Fig. 3. Unlike canvas data similar findings are obtained for these data too. Considering the histograms of the intensity inhomogeneity corrected results it may be concluded that the proposed scheme is providing better results. The last examples we have considered is of 3T images and is taken from the NCI-ISBI-2013 challenge database. All the MRIs are selected from Prostate Diagnosis and Prostate-3T collections on TCIA. The cases consist of axial scans of the object. We have considered one MRIs of the said database. Analysis of the results as shown in Fig. 4, reveals that the proposed scheme is found to be providing better results as compared to the other considered techniques.

B. EVALUATION OF PERFORMANCE METRICS

To provide a quantitative evaluation of the proposed scheme, we have used three performance evaluation measures. The considered measures are three indirect performance evaluation measures: coefficient of variation of white matter (CV_{WM}), coefficient of variation of gray matter (CV_{GM}) and the coefficient of joint variation (CJV) [29]. For a better intensity inhomogeneity correction technique, it is required that a smaller CV and CJV is obtained. Obtained results for different MRIs are provided in tabular form. The measures CV(GM), CV(WM) and CJV for these MRIs are put in Tables 1 – 4. All the results reported from BRAINWEB database in section "Visual Analysis of Result" are reported in Table 1 and for other considered BRAINWEB data are provided in Table 3. The results reported for "4RTNI@LONI" database in section "Visual Analysis of Result" are reported in Table 2 and other results of the same database are reported in Table 4. It can be seen from these tables that a smaller value of these measures are obtained by the proposed scheme as compared to other considered existing state-of-the-art techniques.

C. DISCUSSION AND FUTURE WORK

The results produced by the proposed scheme were obtained using the best α values according to trial and error. Here α controls the smoothness of segmentation. A larger penalty for inhomogeneity may be incurred for a higher value of α. A smaller value of α increases the degree of smoothness

TABLE 4. Performance evaluation measures for other "4RTNI LONI" data

Techniques	Canvas15			Canvas 25			Canvas 60		
	CV(GM)	CV(WM)	CJV	CV(GM)	CV(WM)	CJV	CV(GM)	CV(WM)	CJV
Original	0.2010	0.1847	1.7274	0.1812	0.1055	1.4516	0.1996	0.0873	1.0809
EMin	0.1907	0.1802	1.7009	0.1712	0.0973	1.3813	0.1877	0.0769	1.0973
N3	0.1877	0.1768	1.6869	0.1688	0.0923	1.3636	0.1863	0.0722	1.0913
N4	0.1866	0.1746	1.6860	0.1657	0.0911	1.3332	0.1893	0.0688	1.0873
MFCM	0.1989	0.1826	1.7112	0.1789	0.1021	1.4399	0.193	0.0815	1.0071
LSE	0.1842	0.1711	1.6769	0.1611	0.0878	1.3219	0.1769	0.0613	1.0861
MICO	0.1822	0.1701	1.6741	0.1589	0.0857	1.3034	0.1689	0.0601	1.0815
Proposed	**0.1787**	**0.1673**	**1.5321**	**0.1478**	**0.0801**	**1.2976**	**0.1541**	**0.0573**	**1.0733**

in the restored image. Hence, in the proposed approach the tradeoff between false and missed alarms can be controlled by considering the value of $\alpha = 0.5$. Similarly, the other parameter considered in our experiment is λ. A higher value of this parameter will increase the smoothness in the intensity homogeneity corrected image and a smaller value will increase the texture. In the proposed scheme, with trial and error, λ value is fixed as 5.0. The MAP function of the MRF model is a convex function and need to search a space of $2^{MxNx\tau}$, where MxN is the size of the image and τ is the number of bits used to represents an image. Searching the said space needs a large computational time, hence a good initialization may be required to optimize it faster. In the proposed scheme, we have used fuzzy clustering algorithm for initialization of the label field. The source code for both level set and the MICO schemes are obtained from [30]. Similarly, the source code for the modified FCM is obtained from [31]. In all these considered techniques the results, reported here, are obtained by taking an optimum set of parameter values for different MRIs as reported by the corresponding authors.

In the proposed scheme the intensity homogeneity corrections and segmentation of MRIs are considered in a single MAP framework. The segmentation results reveal the effectiveness of the proposed scheme by segmenting different structures of the MRIs with appropriate boundaries. CV_{GM}, CV_{WM} and CJV are the measures reported in Tables 1-4 are used for the evaluation of segmentation results. This work proposes an intensity inhomogeneity correction scheme by fusion of spatio-contextual MRF model and fuzzy clustering scheme in variable neighborhood searching based framework. In this regard, we have provided some theoretical and experimental validation to corroborate to our findings over the existing algorithms. During the work, we identified several lines of future work. Some of them are pointed out here. We like to develop some intensity inhomogeneity correction techniques using conditional random fields. Further a kernelized FCM scheme may be adhered to for obtaining the MAP. Some framework may be developed for estimating the bonding parameter α.

IV. CONCLUSIONS

In this work, a fuzzy set associated Markov random field (MRF) model with variable neighborhood searching framework is developed for estimating and correcting the intensity inhomogeneity of affected MRIs. In the proposed scheme the intensity inhomogeneity correction and segmentation is considered as a combined task. Here the observed MRI is considered to be affected by intensity inhomogeneity and is assumed to be a multiplicative quantity. The segmentation problem is considered as white/grey matter separation. The combined problem of intensity inhomogeneity correction and segmentation is resolved using the MAP estimation technique. The observed image is modeled with fuzzy set associated Gibbs' MRF and corresponding MAP is obtained using variable neighborhood searching scheme. Experiments are carried out on twenty one MRIs taken from four different databases. Simulation results establish the goodness of the proposed technique. Three performance evaluation measures are used for testing the effectiveness of the proposed scheme. The proposed technique provides a better framework for both intensity inhomogeneity correction and segmentation than the existing state-of-the-art-techniques.

ACKNOWLEDGEMENT

The authors appreciate the thorough and constructive comments provided by the reviewers and the editors on this paper.

REFERENCES

[1] U. Vovk, F. Pernus, and B. Likar, "A review of methods for correction of intensity inhomogeneity in MRI," *IEEE Trans. Med. Imag.*, vol. 26, no. 3, pp. 405–421, Mar. 2007.

[2] C. Huang and L. Zeng, "An active contour model for the segmentation of images with intensity inhomogeneities and bias field estimation," *PLoS ONE*, vol. 10, no. 4, Apr. 2015, Art. no. e0120399.

[3] M. Tincher, C. R. Meyer, R. Gupta, and D. M. Williams, "Polynomial modeling and reduction of RF body coil spatial inhomogeneity in MRI," *IEEE Trans. Med. Imag.*, vol. 12, no. 2, pp. 361–365, Jun. 1993.

[4] R. B. Lufkin, T. Sharpless, B. Flannigan, and W. Hanafee, "Dynamic-range compression in surface-coil MRI," *Amer. J. Roentgenol.*, vol. 147, pp. 379–382, Aug. 1986.

[5] R. Guillemaud and M. Brady, "Estimating the bias field of MR images," *IEEE Trans. Med. Imag.*, vol. 16, no. 3, pp. 238–251, Jun. 1997.

[6] B. Likar, M. A. Viergever, and F. Pernus, "Retrospective correction of MR intensity inhomogeneity by information minimization," *IEEE Trans. Med. Imag.*, vol. 20, no. 12, pp. 1398–1410, Dec. 2001.

[7] J. G. Sled, A. P. Zijdenbos, and A. C. Evans, "A nonparametric method for automatic correction of intensity nonuniformity in MRI data," *IEEE Trans. Med. Imag.*, vol. 17, no. 1, pp. 87–97, Feb. 1998.

[8] N. J. Tustison *et al.*, "N4ITK: Improved N3 bias correction," *IEEE Trans. Med. Imag.*, vol. 29, no. 6, pp. 1310–1320, Jun. 2010.

[9] B. M. Dawant, A. P. Zijdenbos, and R. A. Margolin, "Correction of intensity variations in MR images for computer-aided tissue classification," *IEEE Trans. Med. Imag.*, vol. 12, no. 4, pp. 770–781, Dec. 1993.

[10] C. R. Meyer, P. H. Bland, and J. Pipe, "Retrospective correction of intensity inhomogeneities in MRI," *IEEE Trans. Med. Imag.*, vol. 14, no. 1, pp. 36–41, Mar. 1995.

IEEE Journal of Translational Engineering in Health and Medicine

[11] C. Li, R. Huang, Z. Ding, J. C. Gatenby, D. N. Metaxas, and J. C. Gore, "A level set method for image segmentation in the presence of intensity inhomogeneities with application to MRI," *IEEE Trans. Image Process.*, vol. 20, no. 7, pp. 2007–2016, Jul. 2011.

[12] C. Li, J. C. Gore, and C. Davatzikos, "Multiplicative intrinsic component optimization (MICO) for MRI bias field estimation and tissue segmentation," *Magn. Reson. Imag.*, vol. 32, no. 7, pp. 913–923, 2014.

[13] T. Ivanovska *et al.*, "An efficient level set method for simultaneous intensity inhomogeneity correction and segmentation of MR images," *Comput. Med. Imag. Graph.*, vol. 48, pp. 9–20, Mar. 2016.

[14] X. L. Liu, Y. T. Guo, J. Kong, and J. Z. Wang, "A modified fuzzy C-means algorithm brain MR images segmentation with bias field compensation," *Inf. Technol. Appl. Ind., Comput. Eng. Mater. Sci.*, vols. 756–759, pp. 1349–1355, Sep. 2013.

[15] C. Xu, D. L. Pham, and J. L. Prince, "Finding the brain cortex using fuzzy segmentation, isosurfaces, and deformable surface models," in *Proc. Biennial Int. Conf. Inf. Process. Med. Imag.*, 1997, pp. 399–404.

[16] D. L. Pham and J. L. Prince, "An adaptive fuzzy C-means algorithm for image segmentation in the presence of intensity inhomogeneities," *Pattern Recognit. Lett.*, vol. 20, no. 1, pp. 57–68, Jan. 1999.

[17] M. N. Ahmed, S. M. Yamany, N. Mohamed, A. A. Farag, and T. Moriarty, "A modified fuzzy c-means algorithm for bias field estimation and segmentation of MRI data," *IEEE Trans. Med. Imag.*, vol. 21, no. 3, pp. 193–199, Mar. 2002.

[18] W. Cai, S. Chen, and D. Zhang, "Fast and robust fuzzy C-means clustering algorithms incorporating local information for image segmentation," *Pattern Recognit.*, vol. 40, no. 3, pp. 825–838, Mar. 2007.

[19] J. Aparajeeta, P. K. Nanda, and N. Das, "Modified possibilistic fuzzy C-means algorithms for segmentation of magnetic resonance image," *Appl. Soft Comput.*, vol. 41, pp. 104–119, Apr. 2016.

[20] A. Ghosh, B. N. Subudhi, and S. Ghosh, "Object detection from videos captured by moving camera by fuzzy edge incorporated Markov random field and local histogram matching," *IEEE Trans. Circuits Syst. Video Technol.*, vol. 22, no. 8, pp. 1127–1135, Aug. 2012.

[21] S.-G. Kim, S.-K. Ng, G. J. McLachlan, and D. Wang, "Segmentation of brain MR images with bias field correction," in *Proc. APRS Workshop Digit. Image Comput.*, 2003, pp. 3–8.

[22] S. Z. Li, *Markov Random Field Modeling in Image Analysis*. Heidelberg, Germany: Springer, 2001.

[23] B. N. Subudhi, F. Bovolo, A. Ghosh, and L. Bruzzone, "Spatio-contextual fuzzy clustering with Markov random field model for change detection in remotely sensed images," *Opt. Laser Technol.*, vol. 57, pp. 284–292, Apr. 2014.

[24] N. Belacel, P. Hansen, and N. Mladenovic, "Fuzzy J-means: A new heuristic for fuzzy clustering," *Pattern Recognit.*, vol. 35, no. 10, pp. 2193–2200, 2002.

[25] Accessed: 1999. [Online]. Available: http://brainweb.bic.mni.mcgill.ca/brainweb/anatomic ms.html

[26] Accessed: 2018. [Online]. Available: https://ida.loni.usc.edu/

[27] Accessed: 1999. [Online]. Available: http://brainweb.bic.mni.mcgill.ca/cgi/bw/submitrequest

[28] Accessed: 2014. [Online]. Available: https://wiki.cancerimagingarchive.net/display/DOI/NCIISBI+2013+Challenge%3A+Automated+Segmentation+of+Prostate+Structures

[29] M. Ganzetti, N. Wenderoth, and D. Mantini, "Quantitative evaluation of intensity inhomogeneity correction methods for structural MR brain images," *Neuroinformatics*, vol. 14, no. 1, pp. 5–21, Jan. 2016.

[30] Accessed: 2014. [Online]. Available: http://www.engr.uconn.edu/~cmli/

[31] Accessed: 2018. [Online]. Available: http://in.mathworks.com/matlabcentral/fileexchange/25712-bias-field-corrected-fuzzy-c-means/content/BCFCM2D.m